Jurnal Polimesin
Department of Mechanical Engineering
State Polytechnic of Lhokseumawe
http://e-jurnal.pnl.ac.id/polimesin
e-ISSN : 2549-1999 No. : 5 Month : October
p-ISSN : 1693-5462 Volume : 23 Year : 2025

Processing dates: received on 2025-9-23, reviewed on 2025-10-26, accepted on 2025-10-28 and online availability on 2025-10-31

Distortion and mechanical properties of welded AA5083 aluminum material with friction stir welding

Pujono*, Ipung Kurniawan, Joko Setia Pribadi, Nur Akhlis Sarihidaya Laksana, Roy Aries Permana Tarigan
Department of Mechanical Engineering and Agricultural Industry, Cilacap State Polytechnic, Cilacap 53212, Indonesia
*Corresponding author: poejono07@gmail.com

Abstract

AA5083 series aluminum is one of the primary materials used in ship construction due to its excellent weld-ability in conventional welding processes, such as arc welding. However, similar to other aluminum alloys, the weakness of AA5083 is the occurrence of frost cracking during the welding process, especially in the Heat-Affected Zone (HAZ) and the large amount of distortion. The research was conducted by providing additional treatment in the form of in-situ rolling on Friction Stir Welding (FSW). The in-situ rolling treatment used a single roll positioned directly on the weld area and behind the FSW tool and moving simultaneously with the welding process and with a roll load of 8000 N. The characterization carried out included thermal cycle measurements, microstructure observations, hardness value distribution testing, distortion measurements and tensile testing. The results showed that the largest distortion value occurred in the welded material without additional treatment (as welded) of 2.81 mm, while in the material with additional treatment (mechanical), the distortion value was smaller at 1.1 mm. The mechanical specimen had the best mechanical qualities, with a tensile strength of 225.5 MPa and an average hardness value of 61 VHN, whereas the as-welded specimen's tensile strength was 201.8 MPa. This phenomenon occurs because the specimen, with the addition of in situ rolling, experiences grain refinement, and it seems that this is consistent with the Hall-Petch relationship, $\sigma_y = \sigma_0 + k_y\, d^{-1/2}$. Materials with fine grains are harder and stronger than materials with coarse grains, because fine grains have a larger total grain boundary area to hinder dislocation movement. The tensile fracture position was in the advancing side region, where higher heat input occurred in this region than in the retreating side.

Keywords:
AA5083 series aluminum, friction stir welding, distortion, in situ rolling, tensile strength.

1 Introduction

One of the main materials for ship construction is aluminum alloys such as AA5083. The choice of material for this ship is based on several reasons, namely, AA5083 aluminum is a light metal like other aluminum [1]. Al-Mg alloy type 5083 and Al-Mg-Si alloy type 6082 are the most common and conventional aluminum alloys used in shipbuilding [2]. These alloys have shown themselves to be dependable in both manufacturing and maritime applications. Aluminum alloys may compete with high-strength steel and meet or beyond the minimum yield strength criteria for mild steel, sometimes known as normal strength steel. Aluminum is also very resistant to corrosion.

The trend of shipbuilding productivity has almost matched the productivity of the automotive industry in recent years, and the increasing demand for products such as cars, heavy vehicles, airplanes, trains, and ships has significantly triggered an increase in the demand for aluminum materials. AA5083 aluminum alloy has quite good weld-ability when subjected to conventional welding, such as arc welding. However, like aluminum alloys in general, the weakness of the AA5083 aluminum alloy is the occurrence of frost cracking during the welding process, especially in the Heat-Affected Zone (HAZ). A solid-state welding technology, Friction Stir Welding (FSW) has now been discovered. The FSW process is a suitable welding method for aluminum because it occurs in a solid state and has low heat input, thus preventing the occurrence of hot cracks, porosity, residual stress, and distortion [4].

FSW is an appropriate welding process for aluminum because it prevents hot fractures, porosity, and distortion [3]. The FSW process has various disadvantages, including the welds comparatively low mechanical qualities in comparison to the base metal, as well as the possibility of distortion caused by local heat generated during the welding process. The presence of distortion caused by residual stress can lead to embrittlement, lower fatigue crack development resistance, and the formation of environmentally sensitive cracks (stress corrosion cracking).

To solve this problem, research is needed on welding technology innovation in the form of stress-relieving technology based on the tensioning effect produced by mechanical influence through the provision of pressure rollers (rolling). The addition of a backing plate and the provision of tensile loads (global mechanical tensioning) during the welding process can reduce bending distortion and reduce the residual stress value in FSW welds. This occurs because residual compressive stress appears in the nugget zone [4]. In situ rolling with a two-roll system does not have an effect on the residual stress in FSW welds from aluminium alloy. This may be because the roller is located too far behind the tool [5]. In order to improve the efficacy of this technique, research will be done using either a single roller that is positioned immediately in the weld area and behind the FSW tool, or a roller that moves along the weld line with the tool while the weld metal is still soft. The effect of in situ rolling treatment on the physical and mechanical properties of FSW welded joints of AA5083 aluminum alloy material will be studied in this study, so that this study becomes the best alternative in order to control distortion and the mechanical properties of the welding results.

The workpiece has a propensity to distort as a result of solidification brought on by thermal shrinkage and contraction of the weld metal during welding. There is a possibility that the welded workpiece will shrink both longitudinally and transversely along the intersection. Welding from the top of the workpiece typically results in upward angular distortion. Because the top of the weld is typically wider than the bottom, there is greater shrinkage compaction and thermal contraction there [6].

As a result, the resulting angular distortion is upward. Several methods can be used to reduce distortion; pre-setting is done by estimating the number of distortions that may occur during welding and then welding to compensate for the distortion, this is also known as the material layout method; elastic respringing can reduce angular distortion after the material is released. Preheating thermal settings during welding, as well as providing a tensioning effect in the form of rolling, and heating post-weld, can also reduce angular distortion. Distortion control can also be done by performing balance welding in the form of a double V profile weld [7].

2 Research methodology

The study material employed is an AA5083-type aluminum alloy plate with a thickness of 3 mm, a length of 30 cm, and a width of 20 cm. The AA5083 aluminum alloy material was joined using friction stir welding with the addition of in-situ rolling treatment (mechanical) and without the addition of in-situ rolling treatment (as welded). Table 1 displays the chemical composition of the aluminum alloy plate from the AA5083 series.

Table 1. Chemical composition (wt%)

AA5083 aluminum series	
Element	% wt
Silicon	0.4
Cuprum	0.1
Ferro	0.4
Magnesium	4.0-4.9
Mangan	0.4-1.0
Cromium	0.05-0.25
Ti	0.15
Zn	0.25
Al	Bal.

A milling machine with a V of 60 mm/min and N of 1500 rpm was used to execute FSW. The tool profile had a shoulder dia. of 14 mm, a pin with a dia. of 5 mm, and a pin length of 2.8 mm. The tool was constructed from AISI H13 series tool steel. In Fig. 1, the tool geometry is displayed.

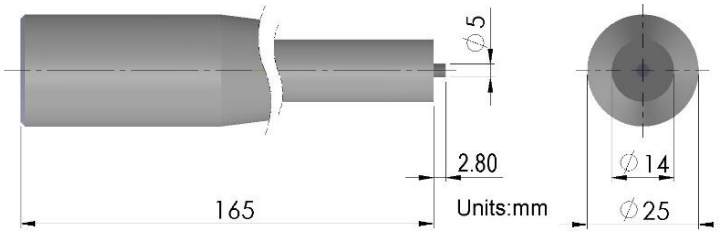

Fig. 1. Geometry tool.

In the FSW process, the tool is tilted towards the vertical axis at an angle of 2°-4°. The treatment added to this FSW process is mechanical tensioning in the form of in-situ rolling with a roll load of 8000 N. The FSW process concept is presented in Fig. 2.

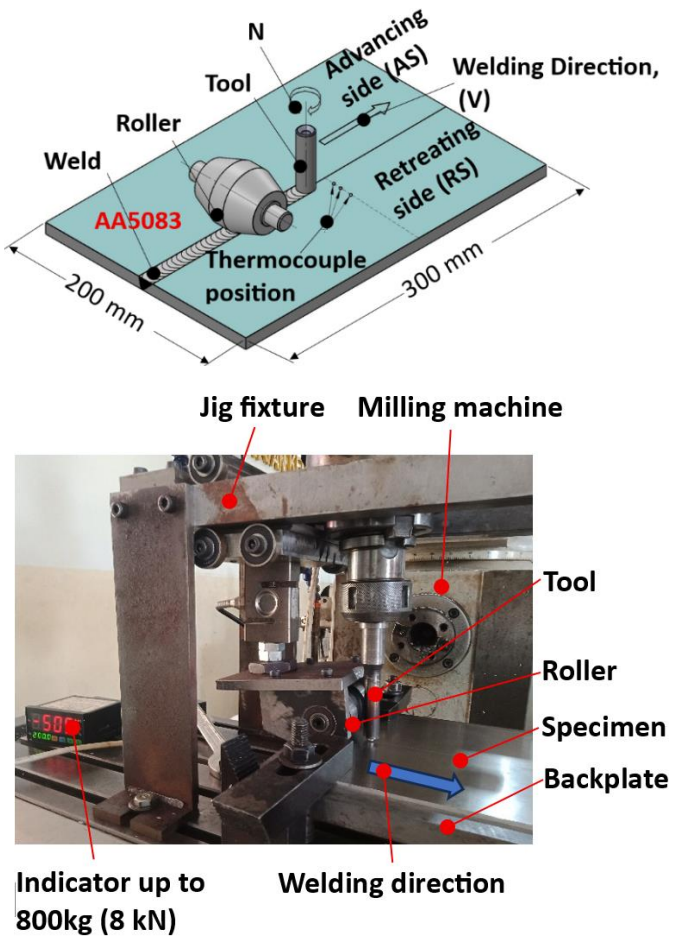

Fig. 2. FSW process scheme with in situ rolling treatment.

In the in-situ rolling process, the roller is placed behind the tool and directly above the weld area; the tool and roller move together in the welding direction.

The welding thermal cycle significantly affects the weld microstructure, which impacts the mechanical properties of the weld [8]. Furthermore, temperature differences during expansion and contraction during the welding process, along with temperature gradients around the weld area, can cause residual stresses and distortion, which can affect the quality of the welded joint.

Peak temperatures were measured in the transverse direction with a K-type thermocouple at distances of 10, 17, and 25 mm from the weld centerline. The purpose of thermal cycle measurement is to determine the rate of heating and cooling during the welding process. A carbon steel base plate was employed during the welding operation and placed beneath the weld material.

Microstructure observations were performed on the sample from the cross-section of the welding area. The purpose of observing the microstructure is to determine the microstructure profile in each welding area, where the microstructure of the welding results affects the mechanical properties of the welding. Before conducting microstructure observations, the specimen surface must be leveled and smoothed with sandpaper from coarse to fine (5000), polished to a shine, and then etched with Keller reagent liquid [9]. With a magnification of 200×, observations were made with an optical microscope in each welding area. Measurements of the distribution of hardness values were carried out using the microVickers test method. Measurements were taken from the cross-section of the welding area, starting from the base metal across the welding area to the base metal again. The load used was 100 grams, and the dwell time was 10 seconds. An illustration of the specimen for microVickers hardness measurement is shown in Fig. 3. The sample size is 60 mm long and 3 mm thick (according to plate thickness). The distance between measurement points is 500 µm, which is measured starting from BM, HAZ, TMAZ, NZ, and BM.

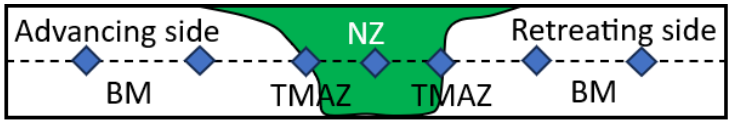

BM : Base metal
TMAZ : Thermomechanically affected zone
HAZ : Heat affected zone
NZ : Nugget zone

Fig. 3. Illustration of the microVickers hardness test.

Tensile test samples were collected from the side perpendicular to the welding region. Fig. 4 depicts the profile and dimensions of the tensile test specimens manufactured in accordance with ASTM E8 criteria. Tensile testing was conducted three times on each specimen. The goal of hardness and tensile testing is to identify the mechanical qualities of welding outcomes.

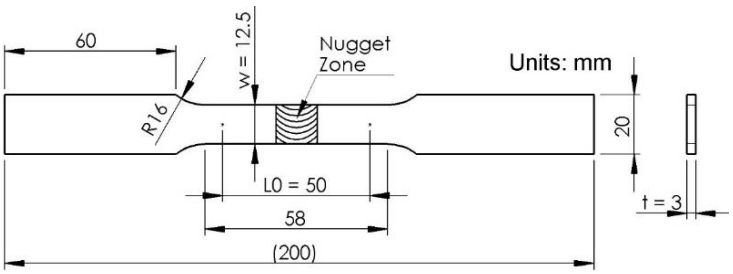

Fig. 4. Tensile test specimen.

3 Results and discussion

The FSW process, without additional treatment and with additional in-situ rolling treatment, has been used in this study. Thermal cycle, distribution of hardness values, macro and micro structures, and tensile strength of the material are the main results of this study. The welding profile of the friction stir welding results is shown in Fig. 5. From Fig. 5, it can be seen that good joining occurs between the two plates welded by friction stir welding.

Fig. 5. FSW process result profile.

3.1 Thermal cycle

During friction stir welding, the weld material goes through a quick temperature cycle that includes both heating and cooling. The deformation, microstructure, and mechanical properties of the weld are all linked to the temperature cycles that occur during the FSW process. Thermal data and peak welding temperatures in the FSW process vary with tool rotation speed. The greater the friction area between the tool and the specimen, the higher the heat input. Friction and plastic deformation in the weld region influence the heat-generating process.

The characteristics of the base metal at high temperatures, the coefficient of friction, and the material flow are also closely related [10]. The results of the thermal cycle measurements are shown in Fig. 6. The peak temperature produced at a measurement distance of 10 mm from the weld centerline is 255ºC.

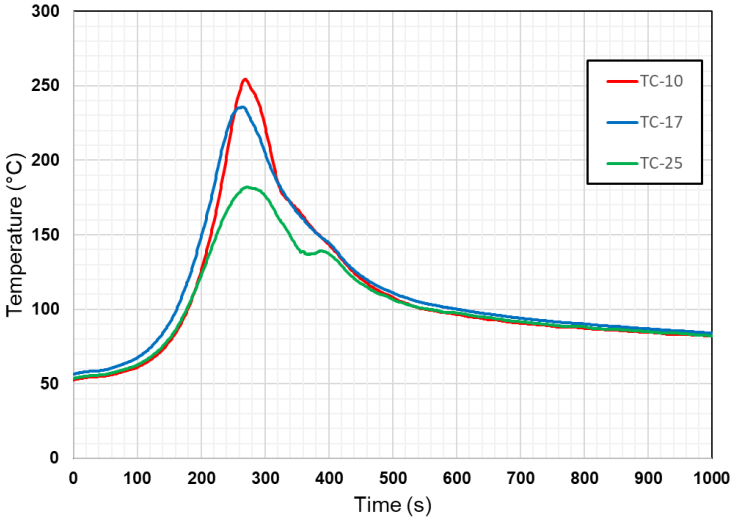

Fig. 6. Thermal cycle measurement results.

3.2 Measurement distortion

The distortion that occurs in the FSW process is relatively small, with the maximum distortion value in the as-welded specimen being 2.70 mm, while in the mechanical specimen it is 1.1 mm. Temperature gradients surrounding the weld region and its surroundings, as well as variations in temperature during expansion and contraction during the welding process, can result in residual stresses that degrade the quality of the welded connection [11]. Heat input from the FSW process causes a high temperature gradient, but with the addition of in-situ rolling treatment, the thermal will be localized due to the tensioning effect. This has an impact on the low distortion that occurs due to welding. The results of this study are in line with [4], that the addition of a backing plate and the application of a tensile load (global mechanical tensioning) during the welding process can reduce bending distortion and reduce the value of residual stress in FSW welds. This occurs because residual compressive stress appears in the weld area. The results distortion measurements are shown in Fig. 7 and Fig. 8. These results indicate that the addition of in-situ rolling treatment can reduce the amount of distortion that occurs in the welded specimens. The amount of this distortion is related to the stress depreciation direction, longitudinal the size is expressed by Eq. (1) [12].

$$\sigma_s = \mu l \frac{\alpha q_w}{\rho c A} E \quad (1)$$

The profile of the distorted welding specimen can be seen in Fig. 9.

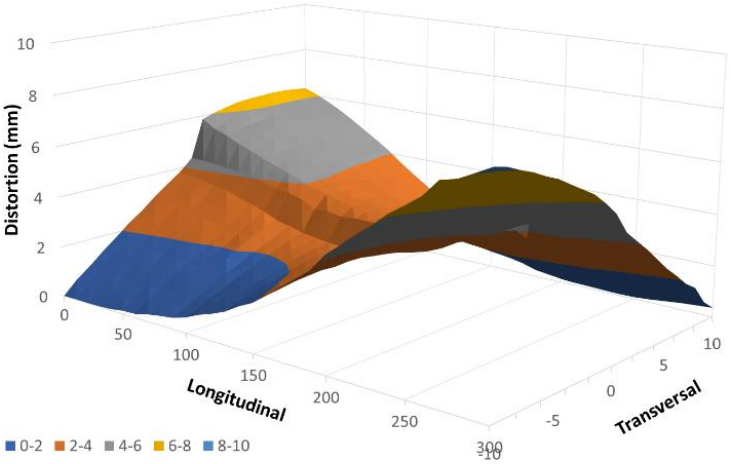

Fig. 7. Distortion of the as-welded specimen.

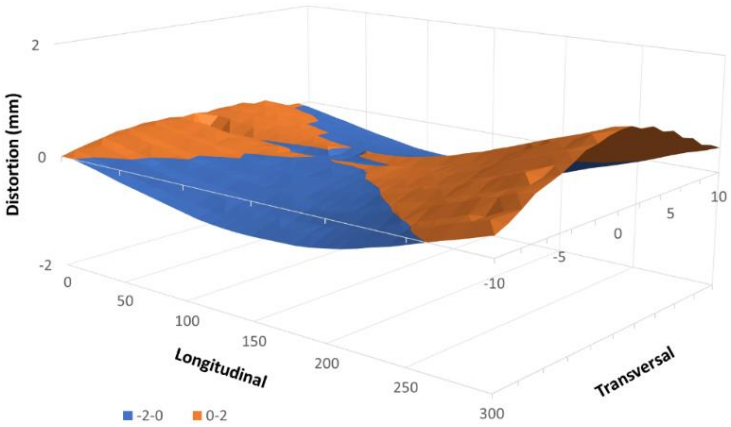

Fig. 8. Distortion of the mechanical specimen.

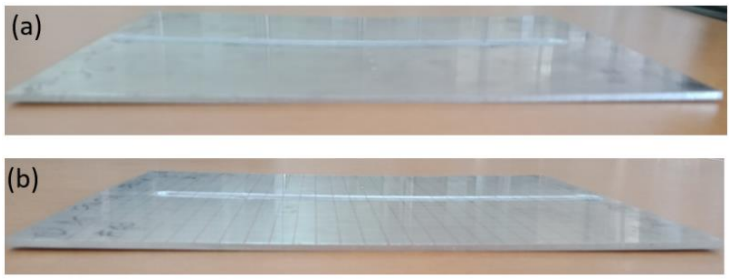

Fig. 9. Distortion profiles; (a) as welded; (b) mechanical.

3.3 Observation macro and micro structure

The results of the macrostructure test showing the welding areas can be seen in Fig. 10. In Fig. 10, it can be seen that each weld zone consists of base metal, heat-affected zone, thermo-mechanically affected zone, and nugget zone. The welding profile forms a trapezoid, and differences in the shape of the microstructure are visible in each welding area. The grains in the weld area show an equiaxed grain shape. The weld profile shows full penetration, proving that the heat from friction between the tool and the material in the FSW process is able to produce sufficient heat input to join the AA5083 aluminum plates. This also explains why the shoulder has a primary function in the metal flow produced by the FSW process [13].

Fig. 11 shows the results of microstructure observations in the HAZ, TMAZ, and NZ weld areas for all specimens. The microstructure in the HAZ area has a larger and coarser grain profile; in this area, recrystallization has not occurred, and the front side usually has a separation between the TMAZ and NZ areas [14]. The microstructure in the NZ area without in-situ rolling treatment is characterized by the presence of a fine-grained polygonal structure that occurs due to dynamic recrystallization during welding. In general, all microstructures show a fine equiaxed shape or fine polygonal grains, which are the result of dynamic recrystallization during the welding process as previously studied [15][16].

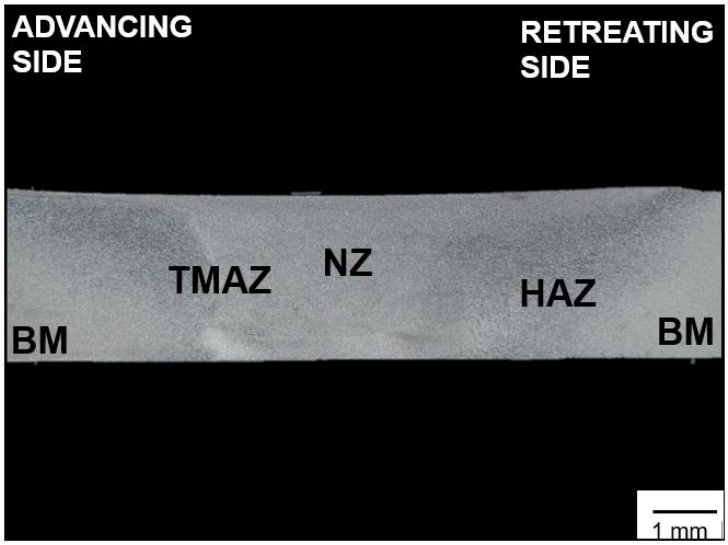

Fig. 10. FSW process areas.

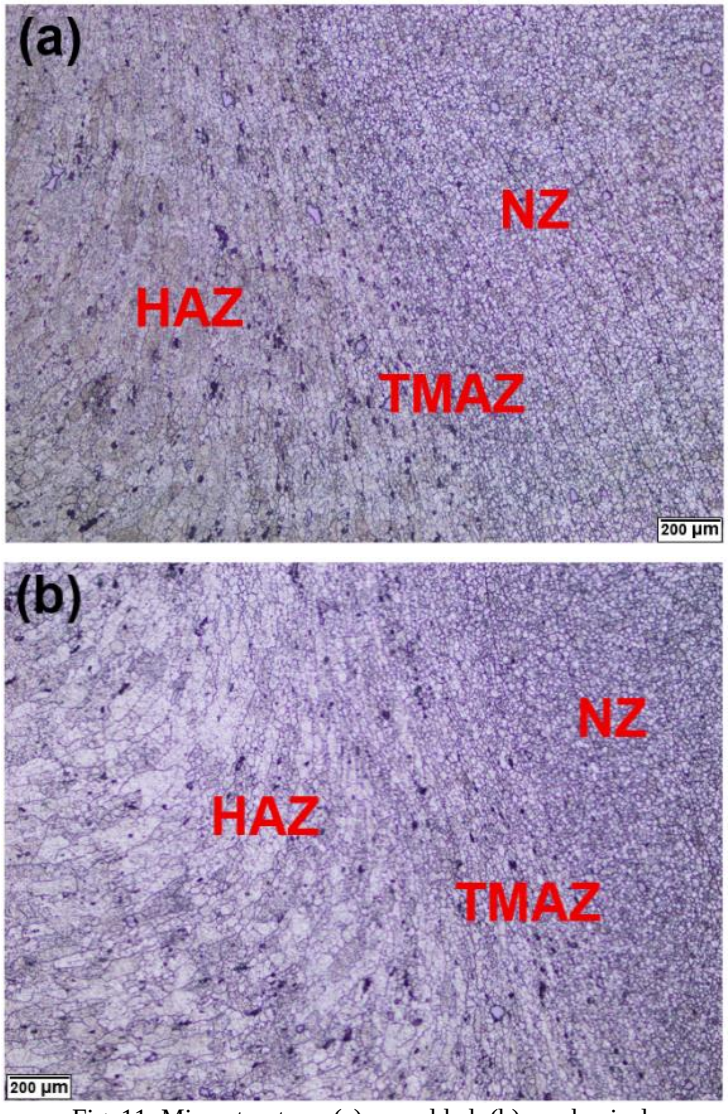

Fig. 11. Microstructure; (a) as welded; (b) mechanical.

The nugget zone is the deepest weld area and the location of the pin rotation during welding. This area has the largest plastic deformation and the highest temperature levels. The grain size of the nugget zone is significantly lower than that of the base metal, which can be attributed to the influence of pin rotation on deformation and grain recrystallization in the stir zone. The TMAZ zone has a coarser microstructure and undergoes plastic deformation due to shear generated by tool rotation and movement. Recrystallization is rarely observed in the TMAZ region due to insufficient deformation and strain. The microstructure in this location differs from the base metal, and the effect of rotational flow with grains extending upward is plainly visible. The HAZ region comes after the TMAZ region. The grains in this region are relatively coarse and undergo thermal cycling, but do not flex plastically during welding. The HAZ has modest microstructural variation when compared to the nugget and TMAZ sections, and the grains are comparable to the base metal structure [17].

3.4 Hardness measurement results

Hardness testing using the microVickers method is carried out on the cross-section. Transverse weld with a distance between points of 500 µm and a load of 100 grams. Distribution of hardness values tends to show a U shape. The results of the hardness test are shown in Fig. 12. From the figure, it can be seen that the weld profile is in the shape of the letter "U" where in the HAZ area there is a decrease in hardness until the minimum hardness is achieved in the TMAZ area, and then there is a slight increase in the hardness value in the NZ area. The hardness value of the NZ area in the specimen with the addition of in-situ rolling (mechanical) is slightly higher than the hardness value of the NZ area in the as-welded specimen. This is the effect of the in-situ rolling treatment, which is a cold working process. The average hardness value in the NZ area is 61 VHN, while in the base metal area it is 90 VHN.

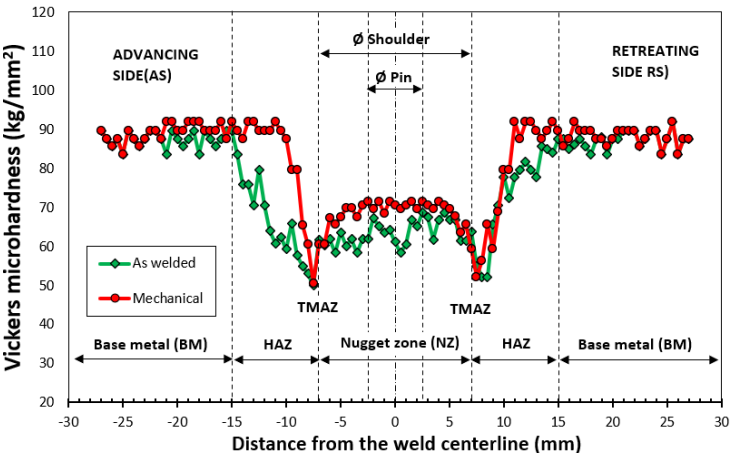

Fig. 12. Distribution of hardness values.

3.5 Tensile test results

The FSW process specimen with in situ rolling (mechanical) treatment had the maximum tensile strength value, 225.5 MPa, while the as-welded specimen had a tensile strength of 201.8 MPa. The tensile strength value of the specimen without in-situ rolling is consistent with prior findings [18]. The tensile test results are shown in Fig. 13.

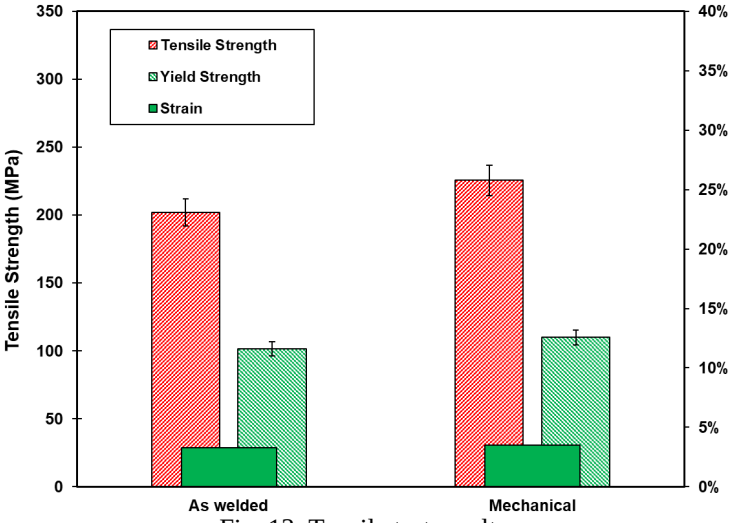

Fig. 13. Tensile test results.

Based on the research results, it can be concluded that the FSW process specimens with the addition of in situ rolling treatment

with a tool rotation of 1500 rpm and a welding speed of 60 mm/minute have the best mechanical properties among the other specimens. The tensile test fracture occurred around the Advancing Side (AS) area as shown in Fig. 14.

Fig. 14. Fracture profile of tensile test results.

The specimen with the highest tensile strength value, 225.5 MPa or 78% of the tensile test value on the base metal, was produced on the FSW-welded specimen with the addition of in-situ rolling treatment. This figure is within the range of FSW welded tensile strength values, which are usually around 75% of the tensile strength of the base metal [19]. The addition of in-situ rolling treatment with a load of 8000 N appears to be able to make the grain size finer than the grains in the as-welded specimen, although it was not too significant. These tensile test results are consistent with the Hall-Petch relationship, which states that the yield strength, σ_y of the metal decreases with increasing grain size (d) as formulated by Eq. (2) [20].

$$\sigma_y = \sigma_0 + k_y\, d^{-1/2} \tag{2}$$

Fig. 15 shows the Scanning Electron Microscope (SEM) fractography results of the fracture surface of the tensile test results. The fracture surface of the FSW-welded joint specimen with a tool rotation of 1500 rpm shows a smooth dimple. Intergranular or facet fractures can be observed in Fig. 15. This can be attributed to the texture caused by the pressing effect of the shoulder on the tool during the FSW process. Some dimples indicate the presence of coarse particles or deposits within them. The appearance of such fractures seems to confirm that the fracture occurs through the coalescence of microvoids [21]. Under these conditions, microvoids can form in coarse deposits because these deposits are more brittle than the α-Al matrix. Then the microvoids become larger and coalesce to form cracks parallel to the stress direction. This can be attributed to the texture caused by the rolling effect during the in-situ rolling process in the FSW process.

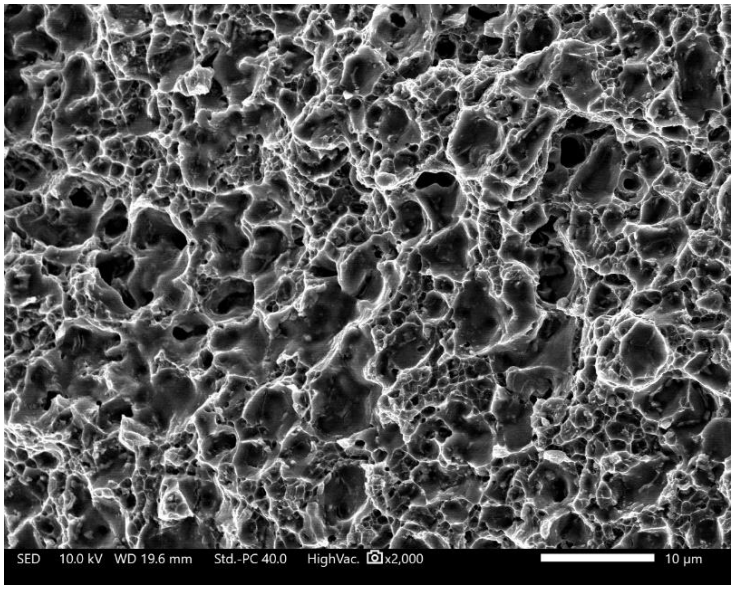

Fig. 15. Tensile test fracture fractography.

4 Conclusions

Research on AA5083 aluminum welding using friction stir welding method without additional treatment (as welded) and with the addition of in situ rolling treatment (mechanical) can be concluded that FSW with the addition of in situ rolling treatment can improve the mechanical properties of the welding results as evidenced by the increase in hardness value and tensile strength value of the welded specimen. The tensile strength value of the as-welded specimen is 201.8 MPa, while the tensile strength value of the mechanical specimen is 225.5 MPa. The addition of in situ rolling treatment is also able to reduce the distortion value in the welded specimen. The lowest distortion occurs in the mechanical specimen, namely 1.1 mm, while in the as-welded specimen, there is a distortion of 2.81 mm.

Acknowledgement

The researcher would like to express his gratitude to Cilacap State Polytechnic for the funding provided for this research through the Internal Research Fund with contract number 135/PL43/AL.04/2025 dated July 23, 2025.

References

[1] Al-Roubaiy, A. O., Nabat, S. M., dan Dl Batako, A, 2019, An Investigation into Friction Stir Welding of Aluminium Alloy 5083-H116 Similar Joints, Materials Today: Proceedings, 22, 2140–2152, https://doi.org/10.1016/j.matpr.2020.03.281.

[2] Koumoulos, E.P., Charitidis, C.A., Daniolos, M.N., Pantelis, D.I., 2013, Determination of onset plasticity (yielding) and comparison of local mechanical properties of friction stir welded aluminum alloys using the micro and nano indentation techniques, International Journal of Structure Integruty. Vol 4. No 1 pp 143-158.

[3] Li, Yingli, Yan, H., Chen, J., Xia, W., Su, B., Ding, T., dan Li, X., 2020, Influences of welding speed on microstructure and mechanical properties of friction stir welded Al-Mg alloy with high Mg content, Materials Research Express, 7(7), 76506. https://doi.org/10.1088/2053-1591/ab9854,

[4] Altenkirch, J., Steuwer, A., Peel, M. J., Withers, P. J., Williams, S. W., dan Poad, M, 2008, Mechanical tensioning of high-strength aluminum alloy friction stir welds, Metallurgical and Materials Transactions A: Physical Metallurgy and Materials Science, 39(13), 3246–3259. https://doi.org/10.1007/s11661-008-9668-1.

[5] Altenkirch, J., Steuwer, A., Withers, P. J., Williams, S. W., Poad, M., dan Wen, S. W., 2009, Residual stress engineering in friction stir welds by roller tensioning, Science and Technology of Welding and Joining, 14(2), 185–192. https://doi.org/10.1179/136217108X388624.

[6] Kou, S., 2003, Metallurgy Second Edition Welding Metallurgy, Wiley-Interscience, A Jhon Wiley and Son INC Publication, Hoboken, New Jersey

[7] Mathers, G., 2000, Welding of aluminum and its alloys, In Welding of aluminum and its alloys alloys, Woodhead Publishing

[8] Ni, Y., Liu, Y., Zhang, P., Huang, J., Yu, X., 2022, Thermal cycles, microstructures and mechanical properties of AA7075-T6 ultrathin sheet joints produced by highspeed friction stir welding, Mater. Charact. 187 111873.

[9] Liu, F., Zhang, D., 2024, Microstructure and mechanical properties of a recycled aluminum alloy fabricated by consolidation of small pieces, heat treatment and surface engineering, 2024, vol. 6, no. 1, 2345938. https://doi.org/10.1080/25787616.2024.2345938

[10] Wang, F.F., Li, Y. W., Shen, J., Hu, S. Y., dos Santos, J. F., 2015, Effect of tool rotational speed on the microstructure and

mechanical properties of bobbin tool friction stir welding of Al–Li alloy, Materials and Design 86 933–940.
[11] Choudhury, S., Medhi, T., Sethi, D., Kumar, S., Roy, B.S., Saha, S.C., 2020, Temperature distribution and residual stress in friction stir welding process, Mater Today: Proc. 26 2296-2301.
[12] Wibowo, H., Ilman, M. N., Iswanto, P. T, 2016, Analysis of welding heat input on distortion, microstructure and mechanical strength of A36 steel, Jurnal Rekayasa Mesin Vol.7, No.1 Tahun 2016: 5-12.
[13] Ramesh, R., Dinaharan, I., Kumar, R., Akinlabi, E. T., 2017, Microstructure and mechanical characterization of friction stir welded high strength low alloy steels, Materials Science & Engineering A.
[14] Ilman, M. N., Sehono, Muslih, M. R., Wibowo, H., 2020, The application of transient thermal tensioning for improving fatigue crack growth resistance of AA5083-H116 FSW joints by varying secondary heating temperature, International Journal of Fatigue, 133 (December 2019), 105464. https://doi.org/10.1016/j.ijfatigue.2019.105464.
[15] Zhang, J., Feng, X. S., Gao, J. S., Huang, H., Ma, Z. Q., Guo, L. J., 2018, Effects of welding parameters and post-heat treatment on mechanical properties of friction stir welded AA2195-T8 Al-Li alloy, Journal of Materials Science and Technology, 34(1), 219–227. https://doi.org/10.1016/j.jmst.2017.11.033.
[16] Robe, H., Zedan, Y., Chen, J., Monajati, H., Feulvarch, E., Bocher, P., 2015, Microstructural and mechanical characterization of a dissimilar friction stir welded butt joint made of AA2024-T3 and AA2198-T3, Mater. Charact. 110 242–251.
[17] Moghadam, D. G., Farhangdoost, K., dan Nejad, R. M., 2016, Microstructure and Residual Stress Distributions Under the Influence of Welding Speed in Friction Stir Welded 2024 Aluminum Alloy, Metallurgical and Materials Transactions B: Process Metallurgy and Materials Processing Science, 47(3), 2048–2062. https://doi.org/10.1007/s11663-016-0611-3.
[18] Bai, Y., Su, H., dan Wu, C., 2021, Enhancement of the Al/Mg Dissimilar Friction Stir Welding Joint Strength with the Assistance of Ultrasonic Vibration, Metals 2021, 11, 1113. https://doi.org/10.3390/met11071113
[19] Zathry, N.E., Mahamood, R.M., Woo, W.L., Green, S., Akinlabi, S., Loganathan, N., and Patel, V., 2025, Comparative evaluation of conventional friction stir welding and ultrasonic vibration-assisted friction stir welding techniques, Journal of Advanced Joining Processes 12 (2025) 100330.
[20] Zhang, L., Liu, C.Y., and Xie, H.Y., 2022, Hall–Petch relation and grain boundary slipping in Al-Mg-Sc alloys with fine equiaxed grain structure, Materials Characterization, Volume 194, December 2022, 112472.
[21] Sun,W., Wang, S., Wu, M., Hong, M., Chen, Y., Xin, J., Yang, P., Qin, Y., Fang, N., 2021, Revealing tensile behaviors and fracture mechanism of Ti–6Al–4V titanium alloy electron-beam-welded joints using microstructure evolution and in situ tension observation, Materials Science and Engineering:A, Volume 824, 8 September 2021, 141811.